Requirement for Fucosyltransferase 2 in Allergic Airway Hyperreactivity and Mucus Obstruction

Naoko Hara[1], Dorota S. Raclawska[1], Leslie E. Morgan[1], James C. NeeDell[1], Lucie Dao[1], Ayako Kato[1], Ana M. Jaramillo[1], Patrick S. Hume[2], Fernando Holguin[1], William J. Janssen[2], Eszter K. Vladar[1], Christopher M. Evans[1]*

[1]Division of Pulmonary Sciences and Critical Care Medicine, Department of Medicine, University of Colorado School of Medicine, Aurora, Colorado, USA

[2]Division of Pulmonary, Critical Care, and Sleep Medicine, Department of Medicine, National Jewish Health, Denver, Colorado, USA

***Corresponding author:**

Christopher M. Evans, PhD
Christopher.evans@cuanschutz.edu
303-724-9287

Keywords: Airways, Mucin, Mucus, Glycosylation, Asthma

Running Title: Fut2 mediated mucus obstruction

Abstract

Mucus hypersecretion is an important pathological problem in respiratory diseases. Mucus accumulates in the airways of people with asthma, and it contributes to airflow limitation by forming plugs that occlude airways. Current treatments have minimal effects on mucus or its chief components, the polymeric mucin glycoproteins MUC5AC and MUC5B. This treatment gap reflects a poor molecular understanding of mucins that could be used to determine how they contribute to airway obstruction. Due to the prominence of glycosylation as a defining characteristic of mucins, we investigated characteristics of mucin glycans in asthma and in a mouse model of allergic asthma. Mucin fucosylation was observed in asthma, and in healthy mice it was induced as part of a mucous metaplastic response to allergic inflammation. In allergically inflamed mouse airways, mucin fucosylation was dependent on the enzyme fucosyltransferase 2 (Fut2). *Fut2* gene deficient mice were protected from asthma-like airway hyperreactivity and mucus plugging. These findings provide mechanistic and translational links between observations in human asthma and a mouse model, which can help in therapeutic targeting of airway mucus.

Introduction

Respiratory tissues are continuously exposed to inspired particles and potential pathogens whose accumulation can damage delicate gas exchange surfaces. Airway mucus is a critical first line of defense, but mucus can also be detrimental in lung diseases (1-5). In asthma, excessive or abnormal mucus is a common feature across ranges of disease severity (2, 6), and airway mucus plugging is a causative feature in fatal asthma (5, 7). In spite of its well-recognized associations with disease, effective therapies to prevent or reverse the effects of mucus overproduction in asthma are lacking. This treatment gap reflects an incomplete mechanistic understanding of mucus dysfunction at a molecular level (8).

The predominant macromolecules in airway mucus are the gel-forming mucin glycoproteins MUC5AC and MUC5B (8, 9). During synthesis, MUC5AC and MUC5B oligomerize through end-to-end disulfide bond formation, and they also become heavily glycosylated (10). The final products are massive glycopolymers with molecular weights in the mega-Dalton range.

Approximately 80% of mucin mass comprises carbohydrates added to long repetitive serine (Ser) and threonine (Thr) rich stretches of the protein backbone while trafficking through the Golgi apparatus. Initial steps in mucin glycosylation involve addition of N-acetylgalactosamine (GalNAc) to Ser and Thr hydroxyls (Figure 1). N-acetylglucosamine (GlcNAc) and/or galactose (Gal) are then added to O-linked GalNAc to form Core glycan structures. Subsequent glycosylation steps include the addition of more GlcNAc and Gal glycans that form branches and extensions. Ultimately glycosylation can be terminated by addition of sialic acid (Sia) or fucose (Fuc) to Gal.

Diversity in mucin glycosylation has evolved in part to mediate host interactions with microbes that recognize specific glycan structures. Although not necessarily mucin isoform specific,

glycosylation does vary across organs with and even within anatomic sub-regions (11). Glycans on mucins also affect the biophysical properties of mucus gels due to effects on osmotic pressures exerted by the mass and charge of linked carbohydrates. Fuc is a relatively non-polar mucin glycan whose polar surface area is approximately half of that presented by Sia. Accordingly, mucus that is rich in fucosylated mucin may be highly viscoelastic and prone to aggregation. While thick mucus may be helpful for anti-microbial defense, it can lead to physiologic dysfunction. Indeed, fucose was found to be the most significant determinant of abnormal viscoelasticity in chronic sinusitis mucus (12).

The addition of Fuc to Gal residues on mucins is mediated by the fucosyltransferase enzyme FUT2, which catalyzes formation of a glycosidic bond between the first carbon on Fuc and the second carbon on Gal thereby generating a Fuc(α1-2)Gal structure (hereafter referred to as α-Fuc). This structure is also found on blood group secretor (or H) antigen, and H-positive secretor status increases asthma patients' risks for severe asthma exacerbations (13). We hypothesized that a potential explanation for this may be through FUT2-mediated mucin fucosylation. We tested this by investigating Fut2-mediated mucin fucosylation and its effects on airflow obstruction in a mouse model of allergic asthma.

Methods

Detailed methods are provided in an online supplement.

Human asthma and animal models

Fatal asthma lung samples used for histology were obtained from deidentified tissue donated to National Jewish Health. C57BL/6J congenic *Fut2*$^{-/-}$ mice were generated previously {11713270} and provided by Dr. Justin Sonnenburg at Stanford University. Males and females were used starting at 7-8 wks age. Mice were challenged using aerosolized *Aspergillus oryzae* extract (14) (AOE, 10% w/v; Cat. P6110**,** Sigma, St. Louis, MO) or saline vehicle administered weekly for 4 wks. Endpoints were collected 48 h after the last AOE challenge.

Mucin detection

Triple labeling was performed to detect MUC5AC, MUC5B, and Fuc(α1-2)Gal in human and mouse airways. After antigen retrieval, tissues were blocked with Carbo-Free Blocking Solution (Vector Laboratories, Cat. SP-5040-125).

For human tissues, a mixture containing mouse-anti-human MUC5AC (clone 45M1, Novus, Cat. NBP2-15196, 1:1000 dilution), rabbit-anti-human MUC5B (Sigma, Cat. HPA008246, 1:500 dilution), and biotin-conjugated *Ulex europaeus* agglutinin-1 (UEA1, Vector, B-1065-2, 8 μg/ml) was applied. UEA1 lectin is selective for the glycan structure Fuc(α1-2)Gal (15).

Mouse mucins were detected using polyclonal rabbit-anti-mouse MUC5AC produced against the peptide N-CHALGDTSHAESSEQEFKSKESEEHGQQLAFR (Pacific Immunology, Ramona, CA, 1:2500 dilution), mouse-anti-mouse MUC5B (clone MDA-3E1, Cat. MABT899, MilliporeSigma, Burlington, MA, 1:500 dilution), and UEA1 (as above).

Slides were cover-slipped with fluorescent mounting media containing DAPI. Negative controls

included IgG controls, non-biotinylated UEA1, and knockout mice. Microscopy was performed using an Olympus BX63 microscope and cellSens software (Olympus USA, Center Valley, PA).

Mucin glycoprotein blotting

For mouse lung lavage 5 x 0.5 ml saline was instilled into the right lungs. Aliquots of unmanipulated "neat" lavage fluid were used for leukocyte enumeration or stored at -20° C. For blotting, 27 µl lavage samples were separated on 1% SDS agarose (100 V, 2 h), vacuum transferred to PVDF (16, 17), and blocked with Carbo-Free Blocking Solution (Vector). Mucins were probed with mixtures of UEA1 (1:1,000, 2 µg/ml) and either polyclonal rabbit-anti-mouse MUC5AC (1:2,000) or rabbit-anti-mouse MUC5B (1:5,000) (1, 18). Labels were detected with IRDye 680RD-conjugated streptavidin and IRDye 800CW-conjugated goat anti-rabbit IgG (LI-COR, Lincoln, NE, diluted 1:15,000) using an Odyssey CLx and Image Studio software (LI-COR).

Airway hyperreactivity

As reported previously (14), lung function was measured using a flexiVent (Scireq, Montreal, Quebec, Canada). Mice were anesthetized with urethane (2.0 g/kg, i.p.), tracheostomized, ventilated (150 breaths/min, 10 ml/kg, 3 cm H_2O positive end expiratory pressure) and paralyzed with succinylcholine (10 µg/g/min, i.p.). Total lung resistance (R_L) and airway resistance (R_{AW}) were determined at baseline and in response to nebulized methacholine (MCh; Sigma, St. Louis, MO, Cat no. A2251; 0.1-10 mg/ml).

Mucus plugging

During peak bronchoconstriction, mice were euthanized, and lungs were fixed as described previously (14, 17). Mucins were labeled using alcian blue-periodic acid Schiff's (AB-PAS) stain (19). Total airway vs. parenchyma fractions were counted using a 250 x 250 µm grid, and

airway mucin volume fractions were quantified using a 50 x 50 μm grid. Volume fractions and mucus volumes using were calculated.

Statistical analyses

Statistical analyses were performed using GraphPad Prism 10.2.2 (397). Two-sample comparisons were compared using unpaired two-way *t*-tests or Mann-Whitney U-tests where appropriate. For multiple comparisons, ANOVA with a Dunnett post-hoc correction or a Kruskal-Wallis test with Dunn's post-hoc correction was used.

Results

Mucins are fucosylated in human asthmatic airways and in mouse models of allergic asthma. Mucus plugging is a prominent pathologic feature in fatal asthma. In a histologic sample from a fatal asthma subject, MUC5AC and MUC5B were prominent in goblet cells and in secreted mucus, which also demonstrated strong labeling for fucosylation with the lectin UEA1 (Figure 2A, supplementary Figure E1).

Based on these findings, we tested whether mucin fucosylation was induced in a mouse model of allergic asthma. C57BL/6 mice were exposed to AOE and evaluated for mucin expression and fucosylation histologically. Consistent with findings in human asthma, combined immunofluorescence and lectin labeling showed Muc5ac, Muc5b, and α-Fuc in airway epithelia (Figure 2B, supplementary Figure E2), suggesting a role for Fut2 in regulation of mucin fucosylation.

To investigate a requirement for Fut2, we evaluated effects of *Fut2* gene disruption on airway mucin fucosylation in mice. In wild type (*Fut2*$^{+/+}$) mice at baseline, frequent Muc5b expressing cells were observed with little or no Muc5ac or α-Fuc in the naïve state (Figure 2C). After AOE challenge, allergically inflamed airways showed robust induction of Muc5ac and α-Fuc detection in *Fut2*$^{+/+}$ airway epithelia (Figure 2D). *Fut2*$^{-/-}$ mouse airways had undetectable UEA1 labeling at baseline or after AOE, despite retaining Muc5b and Muc5ac expression (Figure 2E,F). These findings and a prior report showing a detrimental role for FUT2 in humans with asthma (13), prompted us to investigate whether Fut2 absence may protect mice from asthma-like airflow obstruction.

Fut2 is required for airway hyperreactivity in AOE challenged mice. We previously showed in AOE challenged mice that AHR can be abrogated by eliminating mucin from the airways (14, 17). To explore this further, we postulated that Fut2-dependent mucin fucosylation may play an

essential role in causing muco-obstruction during AHR. In AOE challenged *Fut2*$^{+/+}$ mice, airflow obstruction measured by dose dependent increases total lung resistance (R_L) and airway resistance (R_{AW}) in response to MCh inhalation were potentiated compared to measurements in non-allergic controls. These characteristics of allergic asthma-like AHR were abolished in AOE challenged *Fut2*$^{-/-}$ mice (Figure 3).

Findings here are consistent with a previous report in a house dust mite antigen model of asthma (20). In that study, protection of *Fut2*$^{-/-}$ mice from AHR was associated with suppression of epithelial UEA1 labeling and with reduced allergic inflammation. To evaluate these, we compared changes in inflammation and mucin composition in AOE challenged *Fut2*$^{+/+}$ and *Fut2*$^{-/-}$ mice.

Fut2 absence blocks mucin fucosylation but does not affect allergic inflammation in AOE challenged mice. Leukocytes in lung lavage were enumerated, and we observed that AOE strongly induced inflammation in both *Fut2*$^{+/+}$ and *Fut2*$^{-/-}$ mice. Total numbers of leukocytes recovered in lavage fluid and eosinophils specifically were between mutant and wild type (Figure 4A,B). There were also no significant differences in other inflammatory cell types observed (Figure E3).

Protection from allergic AHR despite a lack significant reduction inflammation was similar to prior observations in Muc5ac deficient animals suggesting that protection may relate to direct effects on mucins (14). This stimulated us to investigate whether protection from AHR reflected differences in mucin fucosylation that could affect mucus pathology. Consistent with histologic findings in airway epithelia (see Figure 2), immuno- and lectin blotting showed that both MUC5AC and α-Fuc detection were low in MUC5B-rich mucin collected from naïve mice (Figure 4C). After AOE challenge, there was a strong induction of mucin fucosylation. MUC5B and MUC5AC were both increased and fucosylated. Colocalization of UEA1 signals validated that

mucins themselves carry α-Fuc glycans after AOE-induced allergic inflammation. Mucin fucosylation increases the viscoelasticity of mucus in chronic sinusitis (12), so we hypothesized that Fut2 may potentiate AHR by promoting mucus obstruction.

Mucin fucosylation promotes airway mucus obstruction.

We assessed secreted mucus volume, airway occlusion, and heterogeneous plugging in AOE challenged mice during MCh-induced bronchoconstriction. In *Fut2*$^{+/+}$ mouse airways, secreted mucus aggregated on airway surfaces (Figure 5A), but accumulated mucus was less apparent in airways from *Fut2*$^{-/-}$ mice (Figure 5B). These observations were validated by stereologic quantification. Bronchial mucus volumes and fractional mucin occlusion were significantly decreased in *Fut2*$^{-/-}$ compared to *Fut2*$^{+/+}$ mice (Figure 5C,D).

Overall mean levels of mucus obstruction do not fully reflect the heterogenous nature of mucus obstruction that drives AHR (14, 17). We thus evaluated frequencies of airway occlusion at different magnitudes. Consistent with prior findings in Muc5ac deficient and mucolytic treated mice (14, 17), *Fut2*$^{-/-}$ mice demonstrated significantly greater proportions of airways with 20% or less occlusion (Figure 5E). Thus, Fut2 absence in mice resulted in protection from a heterogeneous muco-obstructive phenotype that is also similar to what is seen in fatal asthma (5).

Discussion

The studies reported here demonstrate that mucin fucosylation is associated with allergic mucous metaplasia (see Figure 2), and it plays a causative role in asthma-like airflow obstruction in mice. A role for FUT2 is supported by findings in *Fut2* gene disrupted mice that lack fucosylated airway mucins and are protected from AHR and airway mucus plugging (see Figures 3-5). These findings provide a translational link to prior reports showing associations between mucin fucosylation in human asthma and animal models (13, 21, 22)

FUT2 and mucin gene loci are linked to chronic sputum production (23), and people with asthma who lack FUT2 are protected from severe exacerbations (13). Over extended periods, these could be explained by effects on host defense and inflammation, which are complex and are likely both organism and tissue specific. Secretor status can affect how hosts respond to viral, bacterial, and fungal microorganisms in different organs.

People with *FUT2* loss-of-function mutations are protected from viral infections including HIV (24, 25), norovirus (26), and rotavirus (27), which use a Fuc(α1-2)Gal carbohydrate linkage for host cell attachment. FUT2 absence is also associated with bacterial infections in the middle ear (28) and the lungs (29), and with the dysbiosis and pathogen infection in the gastrointestinal and female reproductive tracts (30-32). In the intestine, FUT2 helps shape the gut microbiota (30), and type 3 innate lymphoid cells regulate its expression (31). It is possible that gut-derived signals can affect immune tone in distant organs such as the lung.

A connection between Fut2 and the development of allergic inflammation was explored previously (20). In a house dust mite antigen exposure model, *Fut2* deficient mice were protected from AHR, and their airways were devoid of UEA1-positive α-Fuc signals. That report also found that inflammation was partly reduced, including an approximately 50% decrease in lavaged eosinophils. We did not observe a decrease in inflammation in mice challenged with

AOE (see Figure 4A,B). Accordingly, acute inflammosuppression and effects of prolonged FUT2 absence do not account for protection from AHR in findings reported here.

Fungal derived fucose-selective lectins may reveal relevant relationships between type 2 immune signals and the upregulation of mucin fucosylation in the lungs. *Aspergillus fumigatus* expresses a fucose-specific lectin called FleA that binds to mucins (33, 34). *Aspergillus oryzae* expresses a FleA lectin as well (35). FleA-mucin interactions are proposed as important means through which fucosylated mucins support innate host defense by trapping fungal conidia and allowing their elimination by mucociliary clearance (33, 34). This induction of a fucosylated mucous phenotype is consistent with aberrant overlaps observed between protective type 2 immunity and allergy.

Without a need for type 2 mediated immune defense, the acquisition of a heavily fucosylated mucin glycotype in allergically inflamed lungs results in mucus dysfunction. Fucose is a low charge glycan that increases mucus viscoelasticity. Studies in upper airway tissues from chronic sinusitis patients suggest that mucus rheology is fucose dependent (12). An excessively viscoelastic mucus gel can overwhelm mucociliary or even cough generated clearance forces. In lower airways, the production of MUC5AC and a low-charge glycoform of MUC5B is associated with altered mucin composition in asthma (36, 37), and it is prominent finding in fatal cases (38). These associations could be explained in part as resulting from excessive fucosylation (39) (see Figure 1A), but additional mechanistic work is needed.

Based on our findings, two important next steps are to determine mechanisms that regulate the expression and the function of FUT2. Expression is complex, and studies in mice show that it may reflect tissue specific programs such as IL-22 driven phenotypes in the gastrointestinal tract (31) versus IL-13 mediated regulation in the airways (20). Inflammatory and gene regulation mechanisms may also reflect genetic differences that vary among species. Also

notable is that the associations of *FUT2* and mucin gene loci with chronic sputum production were found in people even without prior respiratory disease diagnoses (23).

Accordingly, another needed area of investigation relates to gaining a better understanding of FUT2 enzymatic activity independent of upstream pathways that regulate *FUT2* expression. Little is known about α1-2 fucosyltransferases structurally, but high-resolution characterizations of a FUT8 have been made (40-43). They reveal crucial sites of GDP-fucose docking and catalysis of N-linked Fuc(α1-6)GlcNAc bond formation. They also identify allosteric sites on FUT8 that mediate its activity, especially with respect to its function in the low pH environment of the Golgi apparatus.

In summary, mucus obstruction plays pathological roles in asthma and other pulmonary diseases. Presently, there are no effective drugs that specifically target mucins. The findings reported here demonstrate a detrimental role for FUT2-mediated fucosylation in mucus obstruction. FUT2 inhibition is presently limited to utilization of non-selective modified fucose derivatives (44), but FUT2 selective antagonists are being developed for treating cancer (45). A deeper understanding of *FUT2* gene regulation and FUT2 structure-function relationships may guide development of specific inhibitors.

References

1. Roy MG, Livraghi-Butrico A, Fletcher AA, McElwee MM, Evans SE, Boerner RM, et al. Muc5b is required for airway defence. Nature. 2014;505(7483):412-6. Epub 2013/12/10. doi: 10.1038/nature12807. PubMed PMID: 24317696; PubMed Central PMCID: 4001806.

2. Dunican EM, Elicker BM, Gierada DS, Nagle SK, Schiebler ML, Newell JD, et al. Mucus plugs in patients with asthma linked to eosinophilia and airflow obstruction. The Journal of clinical investigation. 2018;128(3):997-1009. Epub 2018/02/06. doi: 10.1172/JCI95693. PubMed PMID: 29400693; PubMed Central PMCID: 5824874.

3. O'Riordan TG, Zwang J, Smaldone GC. Mucociliary clearance in adult asthma. The American review of respiratory disease. 1992;146(3):598-603. Epub 1992/09/01. doi: 10.1164/ajrccm/146.3.598. PubMed PMID: 1519834.

4. Messina MS, O'Riordan TG, Smaldone GC. Changes in mucociliary clearance during acute exacerbations of asthma. The American review of respiratory disease. 1991;143(5 Pt 1):993-7. Epub 1991/05/01. doi: 10.1164/ajrccm/143.5_Pt_1.993. PubMed PMID: 2024856.

5. Kuyper LM, Pare PD, Hogg JC, Lambert RK, Ionescu D, Woods R, Bai TR. Characterization of airway plugging in fatal asthma. AmJMed. 2003;115(1):6-11. PubMed PMID: 12867228.

6. Ordonez CL, Khashayar R, Wong HH, Ferrando R, Wu R, Hyde DM, et al. Mild and moderate asthma is associated with airway goblet cell hyperplasia and abnormalities in mucin gene expression. American journal of respiratory and critical care medicine. 2001;163(2):517-23. Epub 2001/02/17. doi: 10.1164/ajrccm.163.2.2004039. PubMed PMID: 11179133.

7. Dunnill MS. The pathology of asthma, with special reference to changes in the bronchial mucosa. JClinPathol. 1960;13:27-33. PubMed PMID: 13818688.

8. Fahy JV, Dickey BF. Airway mucus function and dysfunction. The New England journal of medicine. 2010;363(23):2233-47. Epub 2010/12/03. doi: 10.1056/NEJMra0910061. PubMed PMID: 21121836; PubMed Central PMCID: 4048736.

9. Boucher RC. Muco-Obstructive Lung Diseases. The New England journal of medicine. 2019;380(20):1941-53. Epub 2019/05/16. doi: 10.1056/NEJMra1813799. PubMed PMID: 31091375.

10. McShane A, Bath J, Jaramillo AM, Ridley C, Walsh AA, Evans CM, et al. Mucus. Current biology : CB. 2021;31(15):R938-R45. doi: 10.1016/j.cub.2021.06.093. PubMed PMID: 34375594; PubMed Central PMCID: PMC8759706.

11. Becker DJ, Lowe JB. Fucose: biosynthesis and biological function in mammals. Glycobiology. 2003;13(7):41R-53R. Epub 20030319. doi: 10.1093/glycob/cwg054. PubMed PMID: 12651883.

12. Majima Y, Harada T, Shimizu T, Takeuchi K, Sakakura Y, Yasuoka S, Yoshinaga S. Effect of biochemical components on rheologic properties of nasal mucus in chronic sinusitis.

American journal of respiratory and critical care medicine. 1999;160(2):421-6. Epub 1999/08/03. PubMed PMID: 10430708.

13. Innes AL, McGrath KW, Dougherty RH, McCulloch CE, Woodruff PG, Seibold MA, et al. The H antigen at epithelial surfaces is associated with susceptibility to asthma exacerbation. American journal of respiratory and critical care medicine. 2011;183(2):189-94. Epub 2010/08/25. doi: 10.1164/rccm.201003-0488OC. PubMed PMID: 20732988; PubMed Central PMCID: 3040389.

14. Evans CM, Raclawska DS, Ttofali F, Liptzin DR, Fletcher AA, Harper DN, et al. The polymeric mucin Muc5ac is required for allergic airway hyperreactivity. Nature communications. 2015;6:6281. Epub 2015/02/18. doi: 10.1038/ncomms7281. PubMed PMID: 25687754; PubMed Central PMCID: 4333679.

15. Pilobello KT, Agrawal P, Rouse R, Mahal LK. Advances in lectin microarray technology: optimized protocols for piezoelectric print conditions. Curr Protoc Chem Biol. 2013;5(1):1-23. doi: 10.1002/9780470559277.ch120035. PubMed PMID: 23788322; PubMed Central PMCID: PMC4734107.

16. Piccotti L, Dickey BF, Evans CM. Assessment of intracellular mucin content in vivo. Methods in molecular biology. 2012;842:279-95. Epub 2012/01/20. doi: 10.1007/978-1-61779-513-8_17. PubMed PMID: 22259143.

17. Morgan LE, Jaramillo AM, Shenoy SK, Raclawska D, Emezienna NA, Richardson VL, et al. Disulfide disruption reverses mucus dysfunction in allergic airway disease. Nature communications. 2021;12(1):249. Epub 2021/01/13. doi: 10.1038/s41467-020-20499-0. PubMed PMID: 33431872; PubMed Central PMCID: PMC7801631.

18. Zhu Y, Ehre C, Abdullah LH, Sheehan JK, Roy M, Evans CM, et al. Munc13-2-/-baseline secretion defect reveals source of oligomeric mucins in mouse airways. J Physiol. 2008;586(7):1977-92. PubMed PMID: 18258655.

19. Evans CM, Williams OW, Tuvim MJ, Nigam R, Mixides GP, Blackburn MR, et al. Mucin is produced by clara cells in the proximal airways of antigen-challenged mice. Am JRespirCell MolBiol. 2004;31(4):382-94. PubMed PMID: 15191915.

20. Saku A, Hirose K, Ito T, Iwata A, Sato T, Kaji H, et al. Fucosyltransferase 2 induces lung epithelial fucosylation and exacerbates house dust mite-induced airway inflammation. The Journal of allergy and clinical immunology. 2019;144(3):698-709 e9. Epub 20190521. doi: 10.1016/j.jaci.2019.05.010. PubMed PMID: 31125592.

21. Alvarez CA, Qian E, Glendenning LM, Reynero KM, Kukan EN, Cobb BA. Acute and chronic lung inflammation drives changes in epithelial glycans. Front Immunol. 2023;14:1167908. Epub 20230522. doi: 10.3389/fimmu.2023.1167908. PubMed PMID: 37283757; PubMed Central PMCID: PMC10239862.

22. Warren KJ, Dickinson JD, Nelson AJ, Wyatt TA, Romberger DJ, Poole JA. Ovalbumin-sensitized mice have altered airway inflammation to agriculture organic dust. Respiratory research. 2019;20(1):51. Epub 20190307. doi: 10.1186/s12931-019-1015-0. PubMed PMID: 30845921; PubMed Central PMCID: PMC6407255.

23. Packer RJ, Shrine N, Hall R, Melbourne CA, Thompson R, Williams AT, et al. Genome-wide association study of chronic sputum production implicates loci involved in mucus production and infection. The European respiratory journal. 2023;61(6). Epub 20230615. doi: 10.1183/13993003.01667-2022. PubMed PMID: 37263751; PubMed Central PMCID: PMC10284065.

24. Ali S, Niang MA, N'Doye I, Critchlow CW, Hawes SE, Hill AV, Kiviat NB. Secretor polymorphism and human immunodeficiency virus infection in Senegalese women. J Infect Dis. 2000;181(2):737-9. doi: 10.1086/315234. PubMed PMID: 10669366.

25. Kindberg E, Hejdeman B, Bratt G, Wahren B, Lindblom B, Hinkula J, Svensson L. A nonsense mutation (428G-->A) in the fucosyltransferase FUT2 gene affects the progression of HIV-1 infection. AIDS. 2006;20(5):685-9. doi: 10.1097/01.aids.0000216368.23325.bc. PubMed PMID: 16514298.

26. Thorven M, Grahn A, Hedlund KO, Johansson H, Wahlfrid C, Larson G, Svensson L. A homozygous nonsense mutation (428G-->A) in the human secretor (FUT2) gene provides resistance to symptomatic norovirus (GGII) infections. Journal of virology. 2005;79(24):15351-5. doi: 10.1128/JVI.79.24.15351-15355.2005. PubMed PMID: 16306606; PubMed Central PMCID: PMC1315998.

27. Imbert-Marcille BM, Barbe L, Dupe M, Le Moullac-Vaidye B, Besse B, Peltier C, et al. A FUT2 gene common polymorphism determines resistance to rotavirus A of the P[8] genotype. J Infect Dis. 2014;209(8):1227-30. Epub 20131125. doi: 10.1093/infdis/jit655. PubMed PMID: 24277741.

28. Santos-Cortez RLP, Chiong CM, Frank DN, Ryan AF, Giese APJ, Bootpetch Roberts T, et al. FUT2 Variants Confer Susceptibility to Familial Otitis Media. American journal of human genetics. 2018;103(5):679-90. Epub 20181025. doi: 10.1016/j.ajhg.2018.09.010. PubMed PMID: 30401457; PubMed Central PMCID: PMC6217759.

29. Taylor SL, Woodman RJ, Chen AC, Burr LD, Gordon DL, McGuckin MA, et al. FUT2 genotype influences lung function, exacerbation frequency and airway microbiota in non-CF bronchiectasis. Thorax. 2017;72(4):304-10. Epub 20160808. doi: 10.1136/thoraxjnl-2016-208775. PubMed PMID: 27503233.

30. Kashyap PC, Marcobal A, Ursell LK, Smits SA, Sonnenburg ED, Costello EK, et al. Genetically dictated change in host mucus carbohydrate landscape exerts a diet-dependent effect on the gut microbiota. Proceedings of the National Academy of Sciences of the United States of America. 2013;110(42):17059-64. Epub 20130923. doi: 10.1073/pnas.1306070110. PubMed PMID: 24062455; PubMed Central PMCID: PMC3800993.

31. Goto Y, Obata T, Kunisawa J, Sato S, Ivanov, II, Lamichhane A, et al. Innate lymphoid cells regulate intestinal epithelial cell glycosylation. Science. 2014;345(6202):1254009. Epub 20140821. doi: 10.1126/science.1254009. PubMed PMID: 25214634; PubMed Central PMCID: PMC4774895.

32. Domino SE, Hurd EA, Thomsson KA, Karnak DM, Holmen Larsson JM, Thomsson E, et al. Cervical mucins carry alpha(1,2)fucosylated glycans that partly protect from experimental vaginal candidiasis. Glycoconj J. 2009;26(9):1125-34. doi: 10.1007/s10719-009-9234-0. PubMed PMID: 19326211; PubMed Central PMCID: PMC2794911.

33. Kerr SC, Fischer GJ, Sinha M, McCabe O, Palmer JM, Choera T, et al. FleA Expression in Aspergillus fumigatus Is Recognized by Fucosylated Structures on Mucins and Macrophages to Prevent Lung Infection. PLoS Pathog. 2016;12(4):e1005555. Epub 2016/04/09. doi: 10.1371/journal.ppat.1005555. PubMed PMID: 27058347; PubMed Central PMCID: 4825926.

34. Houser J, Komarek J, Kostlanova N, Cioci G, Varrot A, Kerr SC, et al. A soluble fucose-specific lectin from Aspergillus fumigatus conidia--structure, specificity and possible role in fungal pathogenicity. PloS one. 2013;8(12):e83077. Epub 20131210. doi: 10.1371/journal.pone.0083077. PubMed PMID: 24340081; PubMed Central PMCID: PMC3858362.

35. Ishida H, Moritani T, Hata Y, Kawato A, Suginami K, Abe Y, Imayasu S. Molecular cloning and overexpression of fleA gene encoding a fucose-specific lectin of Aspergillus oryzae. Biosci Biotechnol Biochem. 2002;66(5):1002-8. doi: 10.1271/bbb.66.1002. PubMed PMID: 12092808.

36. Welsh KG, Rousseau K, Fisher G, Bonser LR, Bradding P, Brightling CE, et al. MUC5AC and a Glycosylated Variant of MUC5B Alter Mucin Composition in Children With Acute Asthma. Chest. 2017;152(4):771-9. Epub 2017/07/19. doi: 10.1016/j.chest.2017.07.001. PubMed PMID: 28716644; PubMed Central PMCID: 5624091.

37. Kirkham S, Sheehan JK, Knight D, Richardson PS, Thornton DJ. Heterogeneity of airways mucus: variations in the amounts and glycoforms of the major oligomeric mucins MUC5AC and MUC5B. BiochemJ. 2002;361(Pt 3):537-46. PubMed PMID: 11802783.

38. Sheehan JK, Howard M, Richardson PS, Longwill T, Thornton DJ. Physical characterization of a low-charge glycoform of the MUC5B mucin comprising the gel-phase of an asthmatic respiratory mucous plug. The Biochemical journal. 1999;338 (Pt 2):507-13. Epub 1999/02/20. PubMed PMID: 10024529; PubMed Central PMCID: 1220079.

39. Sheehan JK, Richardson PS, Fung DC, Howard M, Thornton DJ. Analysis of respiratory mucus glycoproteins in asthma: a detailed study from a patient who died in status asthmaticus. AmJ RespirCell MolBiol. 1995;13(6):748-56. PubMed PMID: 7576713.

40. Boruah BM, Kadirvelraj R, Liu L, Ramiah A, Li C, Zong G, et al. Characterizing human alpha-1,6-fucosyltransferase (FUT8) substrate specificity and structural similarities with related fucosyltransferases. The Journal of biological chemistry. 2020;295(50):17027-45. Epub 20201001. doi: 10.1074/jbc.RA120.014625. PubMed PMID: 33004438; PubMed Central PMCID: PMC7863877.

41. Jarva MA, Dramicanin M, Lingford JP, Mao R, John A, Jarman KE, et al. Structural basis of substrate recognition and catalysis by fucosyltransferase 8. The Journal of biological chemistry. 2020;295(19):6677-88. Epub 20200327. doi: 10.1074/jbc.RA120.013291. PubMed PMID: 32220931; PubMed Central PMCID: PMC7212660.

42. Garcia-Garcia A, Ceballos-Laita L, Serna S, Artschwager R, Reichardt NC, Corzana F, Hurtado-Guerrero R. Structural basis for substrate specificity and catalysis of alpha1,6-fucosyltransferase. Nature communications. 2020;11(1):973. Epub 20200220. doi: 10.1038/s41467-020-14794-z. PubMed PMID: 32080177; PubMed Central PMCID: PMC7033129.

43. Ihara H, Ikeda Y, Toma S, Wang X, Suzuki T, Gu J, et al. Crystal structure of mammalian alpha1,6-fucosyltransferase, FUT8. Glycobiology. 2007;17(5):455-66. Epub 20061215. doi: 10.1093/glycob/cwl079. PubMed PMID: 17172260.

44. Pijnenborg JFA, Rossing E, Merx J, Noga MJ, Titulaer WHC, Eerden N, et al. Fluorinated rhamnosides inhibit cellular fucosylation. Nature communications. 2021;12(1):7024. Epub 20211202. doi: 10.1038/s41467-021-27355-9. PubMed PMID: 34857733; PubMed Central PMCID: PMC8640046.

45. Zafar H, Atif M, Atia Tul W, Choudhary MI. Fucosyltransferase 2 inhibitors: Identification via docking and STD-NMR studies. PloS one. 2021;16(10):e0257623. Epub 20211014. doi: 10.1371/journal.pone.0257623. PubMed PMID: 34648519; PubMed Central PMCID: PMC8516197.

Figures and Figure Legends

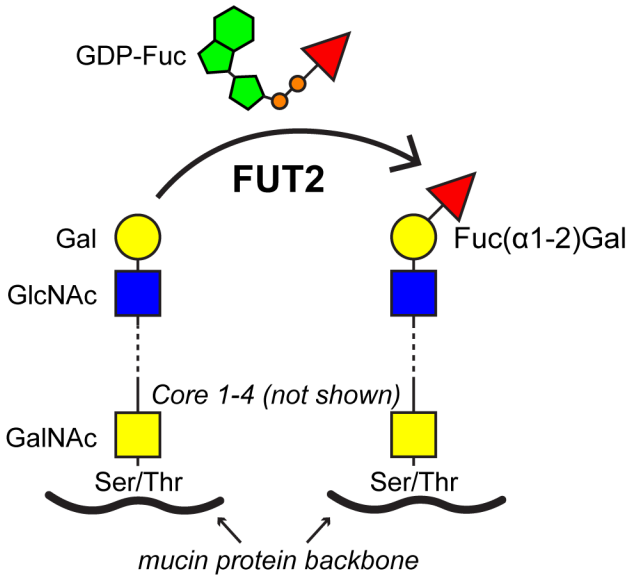

Figure 1. FUT2-mediated mucin fucosylation. Mucin fucosylation occurs via FUT2-mediated attachment of fucose (Fuc, red triangles) to galactose (Gal, yellow circles) glycans that extend from underlying (Ser) or threonine (Thr) residues possessing O-linked N-acetylgalactosamine (GalNAc, yellow squares) with or without N-acetylglucosamine (GlcNAc, blue squares) and Gal extensions. Fuc is transferred from a guanosine diphosphate (GDP)-linked carrier to Gal via bond formation between carbon 1 of Fuc and carbon 2 of Gal, resulting in a Fuc(α1-2)Gal structure.

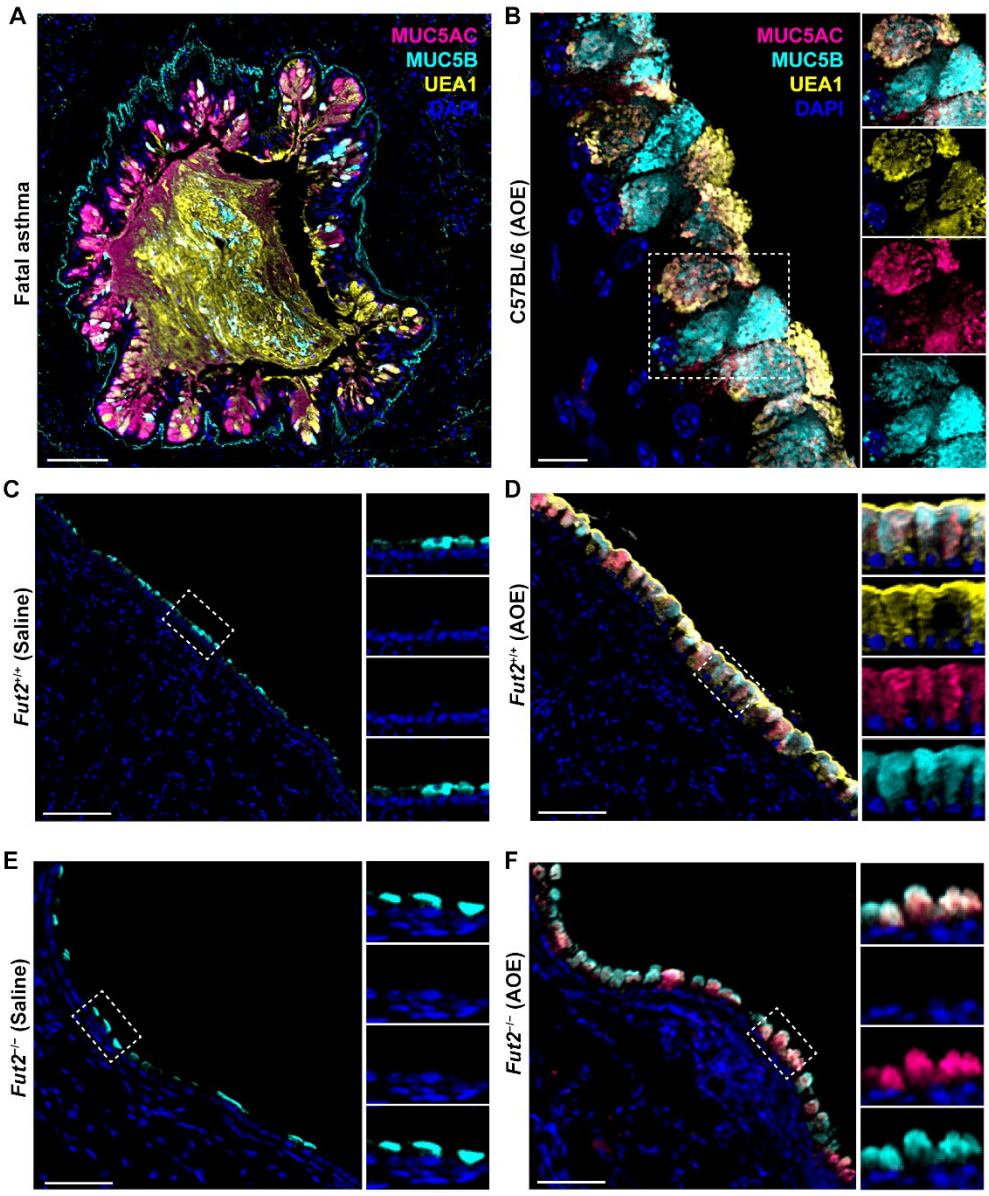

Figure 2. FUT2-mediated fucosylation of airway polymeric mucins in human asthma and in a mouse model. A. α-Fuc was detected using the lectin *Ulex europaeus* agglutinin-1 (UEA1, yellow, 8 μg/ml), which labeled airway mucous cells and a mucus plug in a person who died from fatal asthma. The airway mucins MUC5AC (magenta, 1:1,000) and MUC5B (cyan, 1:500) were both detected. **B-F.** UEA1 labels mouse airway epithelium after induction of allergic inflammation using *Aspergillus oryzae* extract (AOE), and α-Fuc detection is Fut2-dependent. In C57BL/6 mice exposed to AOE (**B**), MUC5B (cyan, 1:500), MUC5AC (magenta, 1:2,500) and α-Fuc (UEA1, yellow, 8 μg/ml) labeling co-localize within airway epithelia. In *Fut2*$^{+/+}$ mice at baseline (**C**), α-Fuc and Muc5ac are not detectable in airway epithelia, but Muc5b is observed. After AOE, Muc5b is sustained while Muc5ac and α-Fuc detection are both induced in *Fut2*$^{+/+}$ animals (**D**). In *Fut2*$^{-/-}$ mice, baseline and AOE-induced expression of Muc5b (**E**) and Muc5ac (**F**) are sustained, but AOE-induced α-Fuc detection is lost (**F**). Nuclei are stained with DAPI (blue). Scale bars: 100 μm for low magnification images and 50 μm for insets in **A** and **C-F**; 10 μm for low magnification image and 8 μm for insets in **B**.

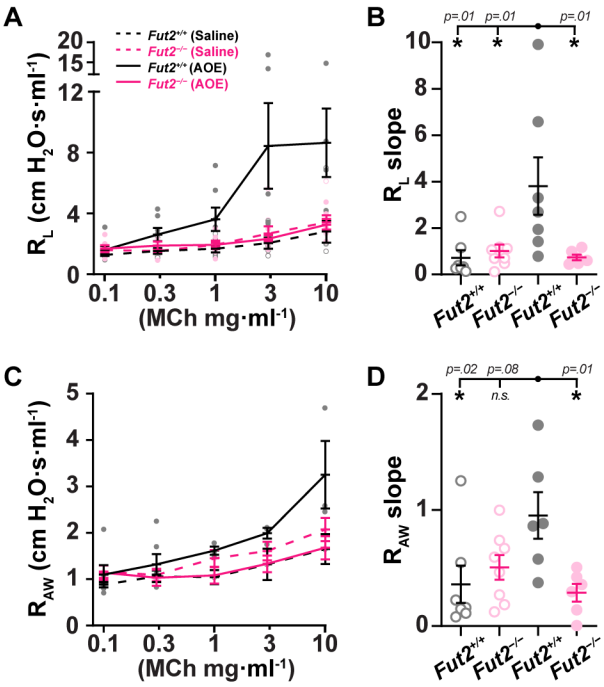

Figure 3. Fut2 is required for allergic airway hyperreactivity. Dose response curves to nebulized methacholine (MCh, 0.1-10 mg/ml) were generated in AOE and saline vehicle challenged *Fut2*$^{+/+}$ (black) and *Fut2*$^{-/-}$ (magenta) mice. Changes in total lung resistance (R_L in **A,B**) and conducting airway resistance (R_{AW} in **C,D**) in response to MCh were measured. Values are means ± sem with individual points per animal depicted by semi-transparent circles. For each animal, dose response curves were fitted by log-linear best-fit regression analysis, and slopes of regression lines were compared by one-way ANOVA. '*', $p < 0.05$ using Dunnett's post-hoc test for multiple comparisons relative to AOE-challenged *Fut2*$^{+/+}$ mice (p-values are shown in **B** and **D**). Comparisons were made between AOE challenged *Fut2*$^{+/+}$ mice (n = 7 biological replicates), AOE challenged *Fut2*$^{-/-}$ mice (magenta, n= 6 biological replicates), saline challenged *Fut2*$^{+/+}$ mice (n = 7 biological replicates for R_L, n = 6 for R_{AW}), and saline challenged *Fut2*$^{-/-}$ mice (magenta dashed lines, n = 8 biological replicates). Solid lines and filled circles identify AOE challenge animals; dashed lines and open circles depict saline challenge controls.

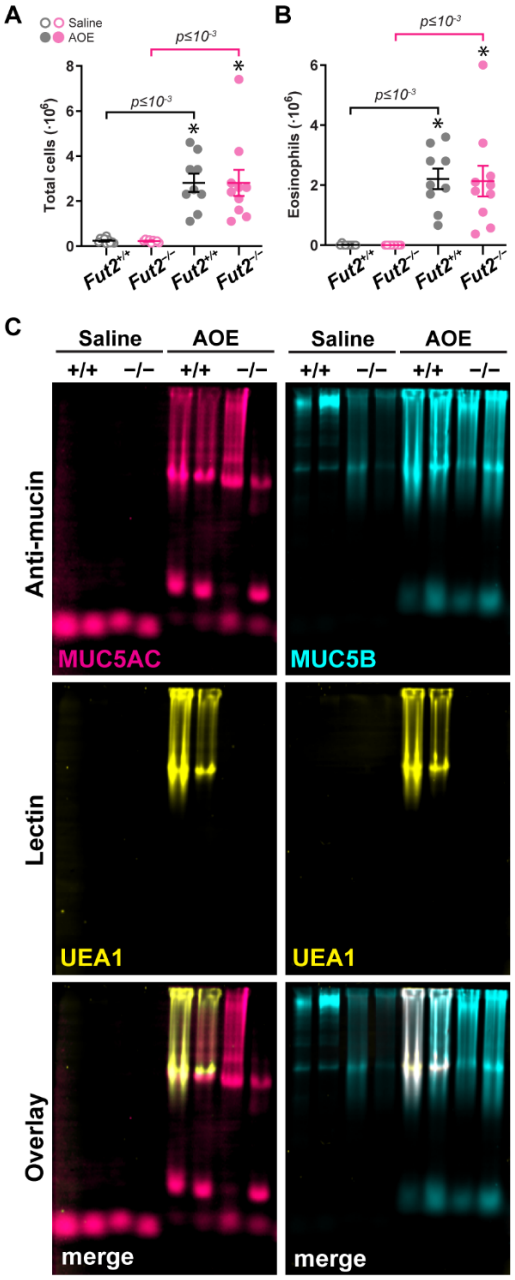

Figure 4. Fut2 deficiency abolishes airway mucin fucosylation but does not reduce inflammation. Lung lavage fluid was obtained from saline and AOE challenged *Fut2*$^{+/+}$ (black) and *Fut2*$^{-/-}$ (magenta) mice. **A,B**. AOE challenge resulted in increases in total numbers of cells (**A**) and eosinophils (**B**), which did not differ between *Fut2*$^{+/+}$ and *Fut2*$^{-/-}$ mice. Data were compared using groups by Kruskal-Wallis ANOVA. '*', $p < 0.05$ using Dunn's post-hoc test for multiple comparisons between genotype and challenge groups (p-values are shown in **A** and **B**). Comparisons were made between AOE challenged *Fut2*$^{+/+}$ mice (n = 9 biological replicates), AOE challenged *Fut2*$^{-/-}$ mice (magenta, n = 10 biological replicates), saline challenged *Fut2*$^{+/+}$ mice (n = 10 biological replicates), and saline challenged *Fut2*$^{-/-}$ mice (magenta dashed lines, n = 9 biological replicates). Solid lines and filled circles identify AOE challenged animals; dashed lines and open circles depict saline challenged controls. **C.** Combined immuno- and lectin blotting was performed on neat lavage. Equal volumes of lavage fluid (27 µl) were loaded per well, separated in 1% SDS agarose gels, and transferred to PVDF membranes. Membranes were probed with biotinylated UEA1 (1:1,000, 2 µg/ml) and either rabbit-anti-MUC5AC (1:2,000) or rabbit-anti-MUC5B (1:5,000). For secondary detection, Alexa 680-conjugated streptavidin and Alexa 800-conjugated labeled goat-anti-rabbit probes (Licor, 1:15,000) were applied. Monochrome images were acquired and pseudocolored magenta (MUC5AC), cyan (MUC5B), or yellow (UEA1). Image overlays demonstrate UEA and mucin signal colocalization (white in merged panels).

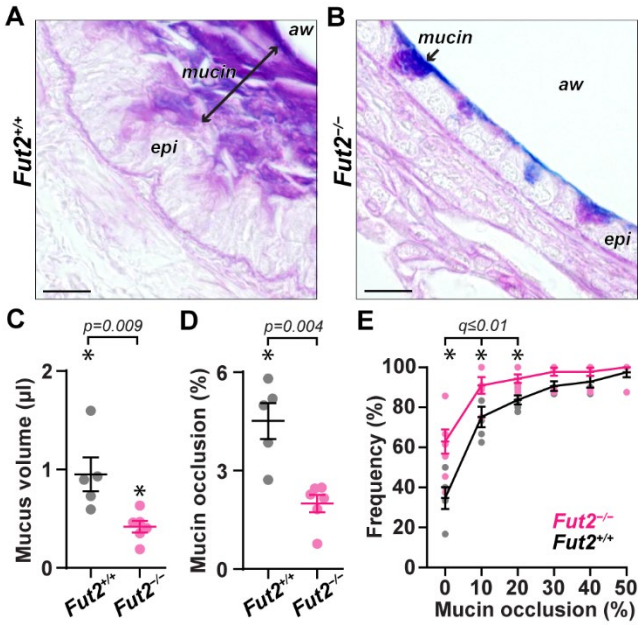

Figure 5. Fut2 deficiency reduces airway mucus plugging. After lung mechanics studies, lungs were fixed with methacarn to preserve mucus in airspaces. **A,B.** AB-PAS stained tissues of *Fut2*$^{+/+}$ mice show mucin aggregated on airway surfaces (**A**) that was less prominent in *Fut2*$^{-/-}$ animals (**B**). Scale bars depict 10 µm; 'epi' is epithelium; 'aw' is airway lumen. **C-E**. Calculated mucus volumes (**C**), fractional mucin occlusion (**D**), and heterogeneous plugging (**E**) were significantly decreased in bronchial airways of AOE challenged *Fut2*$^{-/-}$ mice. Data in **C** and **D** are means ± sem for *Fut2*$^{+/+}$ (black lines, n = 5 mice) and *Fut2*$^{-/-}$ (magenta lines, n = 6 mice) on scatter plots. P-values are shown with '*' depicting $p<0.05$ by two-tailed Mann-Whitney tests. Data in **E** are means ± sem displayed on cumulative frequency distribution graphs. Fractional occlusion means per animal were evaluated between *Fut2*$^{+/+}$ and *Fut2*$^{-/-}$ mice using multiple unpaired t-tests with two-stage step-up methods for multiple comparisons at a false discovery rate cut-off (q-value) set at 0.05. '*' demonstrates significance, and q-values are shown in **E**. Semi-transparent circles identify results from individual mice in **C-E**.